RAPPORT

ANNEE 2022 - 2023

TITRE :
Glacier modelling with Elmer/Ice in relation to Swedish glaciers such as Storglaciären

---

Nom de l'entreprise : Stockholm University (SU)

Adresse : SE-106 91 Stockholm, Sweden

Nom et prénom du Maître de Stage (dans l'entreprise / le laboratoire) :

KIRCHNER Nina

Nom et prénom du Tuteur Ecole

ROUSSEAU Quentin

Stage de :

☐ **1A Découverte de l'Entreprise** **Série** : ☐ A1 ☐ A2 ☐A3 ☐B1 ☐ B2 ☐B3 ☐C1 ☐ C2 ☐C3

☐ **2A Assistant Ingenieur** **Filière :** ☐ ASI☐ HOE☐ GEN ☐ IEE☐ ME ☐ SEM ☐ ADMIS/T ☐ MASTER ☐ ETUDIANTS A L'ETRANGER ☐ AUTRES

X 3A Projet de Fin d'Etudes **Filière :** ☐ ASI☐ HOE X GEN ☐ IEE☐ ME ☐ SEM ☐ MASTER ☐ ETUDIANTS A L'ETRANGER ☐ AUTRES

Nom et prénom de l'étudiant : ROBELIN Olivier

Sujet confidentiel : Oui ☐

Un rapport confidentiel ne pourra être communiqué à quiconque (étudiant, enseignant, personne extérieure) sauf autorisation spéciale accordée par le Maître de Stage dans l'entreprise/le laboratoire

Glacier modelling with Elmer-Ice in relation to Swedish glaciers such as Storglaciren

february - august 2023

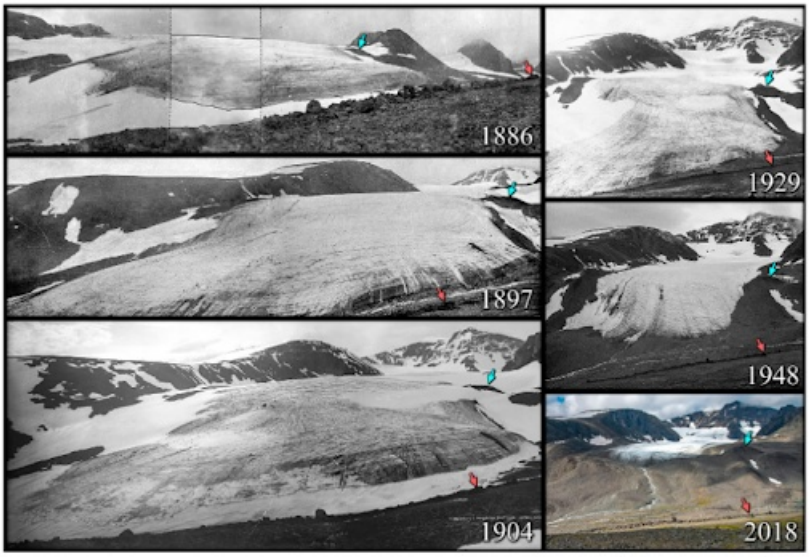

Under the guidance of **Nina Kirchner** from Stockholm University

Olivier ROBELIN
Grenoble INP ENSE3 student

Acknowledgements

At the time of his thanks my first thought goes to Annika Granebeck, station manager of Tarfala Research Station (TRS), victim of a serious leg accident in July 14. We have all been shaken by this painful event. We have missed a lot her dynamism and good humour on a daily basis. With these lines I wish her a good recovery !

I would like to express my sincere gratitude and appreciation to my supervisor Nina Kirchner for giving me the opportunity to study glacier in an Arctic environment. Thank you for trusting me and accepting me as an intern. Thanks also to Jamie Barnett as a co-supervisor for your availability and your expertise.
I would like to thanks Stockholm University (SU) for hosting me on their premises in Stockholm for 4 months and 1 month in TRS. I would like to emphasise on the last month in TRS which was a great experience for me in order to discover Artic field research. Thanks again Nina Kirchner as well as Annika Granebeck for the management of the station and make the science possible in these beautiful landscapes. Proper plant operation is also due to all the awesome staff of the station essential for day-to-day operations and team cohesion, ensuring a spirit of togetherness. Thanks to Maja, Ida, Anders, Perr, Erik for integrating me into the team, having been super kind and hopefully allow me to improve my Swedish. Special thanks to Lisa and Hélène who have ensured that I do not miss French food. This experience will stay in my memories. The field photographs are made possible by Florian's talent as a drone pilot and photographer.
Numerical modelling was possible thanks to the National Academic Infrastructure for Supercomputing in Sweden (NAISS) provided an access to the computational project "Climate Modelling at the Bolin Center for Climate Research (BolinC)."
As a foreign internship in a new place, a good environment is essential for everyday life. Thanks to all the people you met during these 4 months in Stockholm, for these shared moments allowing me a strong Swedish experience. I am thinking in particular of my "camarade" Mathis Darnault for office sharing and so on. Thanks to my roommates Eya and Arthur for having welcomed me to the most beautiful part of the Stockholm suburbs.

The skills required to do this internship have been acquired in Grenoble INP École Nationale Supérieure de l'Énergie l'Eau et l'Environnement (ENSE3). Thanks to my engineering school for these 4 years, the most rewarding in my career, which this internship brings to an end. Thank you to Quentin Rousseau, the school tutor for this internship, who was available and ensured the smooth running of the latter.
Finally, this internship was made possible thanks to funding provided by the Erasmus programme. Thank you Karine Buguet, international mobility department, for advice and administrative formalities.

Glossary

DEM Digital Elevation Model is a representation of elevation data to represent terrain. 6, 10, 12, 19, 24, 25, 28, 29

ELA Equilibrium Line Altitude is a fictive line on a glacier, which represent the transition between the ablation and accumulation area. This fictive line change every year in function of the mass balance. 11, 16, 17, 22, 25, 30

Acronyms

BolinC Bolin Center for Climate Research. 2, 8, 10, 11, 17, 22, 23, 25

ENSE3 École Nationale Supérieure de l'Énergie l'Eau et l'Environnement. 2

FEM Finite Element Method. 7, 9, 14, 18, 29

GPR Ground Penetrating Radar. 10

KTH Swedish Royal Institute of Technology. 8

MUMPS MUltifrontal Massively Parallel sparse direct Solver. 18

NAISS National Academic Infrastructure for Supercomputing in Sweden. 2

SMHI Swedish Meteorological and Hydrological Institute. 8

SU Stockholm University. 2, 7, 8, 32

TRS Tarfala Research Station. 2, 7, 8, 28, 29, 31, 35

WGMS World Glacier Monitoring Service. 12, 17

Contents

List of Figures

List of Tables

Abstract

The 1946-2019 glaciological mass balance series of Storglaciären, northern Sweden, shows a mass loss of the glacier with varying intensity over the time, especially between the 1970s and 1990s when a near-stable mass balance was observed. Using a Finite Element model with a surface DEM, a bed reconstruction of the glacier and by using data collected, a reconstruction of the glacier past evolution was done.
The different behaviours are well reproduced thanks to a deep correlation work between recovered mass balances and their variation in function of the elevation. The model simulated 16.7% of glacier volume lost between 1959 and 2015 whereas 14.7% were observed in the same period by in-situ and satellite data assimilation. Despite this simulated volume lost in 56 years, between 64% and 88% occurred during the period 1999-2015 showing the global trend to obtain negative annual net mass balances. The methodology used for this reconstruction can be used on other alpine glaciers. A mass balance - climate data correlation is needed to explore the future of the small alpine glacier to different climate scenarios.

1 Introduction

The need to produce global climate patterns increased numerical modelling challenges in particular for ice sheets/glaciers modelling where the models were designed for the reconstruction of past-evolution of glaciers (paleoglaciology). Elmer/Ice, parallel Finite Element Method (FEM) was built by the the glaciology community to meet these ambitious goals by solving the full 3D Stokes equations, taking into account short terms responses and providing the possibility to set up local features in a fine mesh which is pretty well adapted to small mountains glaciers such as Storglaciären, very well studied northern Swedish glacier. Thanks to the longest mass balance series of the world which was carried out since 1945, the past evolution of the glacier is known. Many research has been done in order to study the cryosphere in terms of Ice rheology, velocity/sliding as well as mass balance.
Nevertheless, it does not exist a future projection of the glacier evolution subject to climate change. The aim of this study is to use a combination of the dataset collected over time to consider an accurate calibration of a model, and make a reconstruction of the glacier evolution. This calibration can be used as input data for a prognostic run in order to project the evolution according to different future climate scenarios.

The total duration of the internship was 26 weeks, from the 06/02/2023 to the 04/08/2023. The work was divided in the following parts :

- 06/02 - 05/03 : beginning of the internship by remote work from France
- 06/03 - 31/06 : office work at SU laboratory
- 01/07 - 27/07 : field work and visit of TRS
- 28/07 - 04/08 : End of the internship at SU laboratory

In the present report, you will find a presentation of the host organisation. Then, the area of study, data available and the numerical tools used will be described as well as the methodology. After that, we will focus on the results of the simulation and discuss the latter.
In order to describe the field work made during the last month of the internship, an additional section which focus on TRS has been added.

2 Host organisation and numerical tools

2.1 Stockholm University

SU is the biggest university of Sweden with 51 departments each combining research and education. I was hosted by the "Physical Geography" department for this internship. Together with the "Geological Sciences" and "Environmental Sciences" departments, they constitute the "Earth and Environmental Sciences" section, which is part of the academic sciences (see appendix A). The "Earth and Environmental Sciences" research section is located in the Geosciences building, with a staff of 480 including permanent and non-permanent employees (180 for the "Environmental Sciences" department, 130 for the "Physical Geography" department and 70 for the "Geological sciences" department). In practice, around 200 people use the building on a daily basis.

Research topics within the department are varied both in terms of location (figure 1) and subjects of study. This is why different research themes are grouped together in research groups, and I'm part of the "Geomorphology and Glaciology" group, which brings together around fifteen people, mainly from the "Physical Geography" department. This department is headed by Nina Kirchner, researcher and professor of glaciology in the department.

Figure 1: Location of research projects for physical geography department

BolinC is a research group formed by by SU, the Swedish Royal Institute of Technology (KTH) and the Swedish Meteorological and Hydrological Institute (SMHI). It is focus an earth's natural climate system by providing numerical tools. It is the Sweden's strongest centre for inter and multidisciplinary climate research and the modelling project of this internship is part of the BolinC program research.
Nina Kirchner is also my supervisor for this internship. She is also director at TRS, located in Swedish Lapland at the bottom of Storglaciären, the glacier on which my internship is focused. This station is one of the two owned by the department.
I have also worked with Jamie Barnett, a PhD student with Nina (and 2 other researchers) in the Geological Sciences department, working on glacier modelling in Svalbard using Elmer-Ice model. This gives us access to his expertise, as we are using the same modelling tool (see section 2.2). Moreover, he has worked as a research engineer at TRS for field measurements and had the opportunity to initialise a model.

2.2 Elmer-Ice Finite Elment Method

Elmer is an open-source FEM software for multiphysical problems. An extension for Ice Sheet, Glaciers and Ice Flow Modelling was developed and is called Elmer-Ice. It is the main tool used for the present study.
It solves the full-Stokes equations that governed the ice flow for various rheology. The ice is considered as a non-linear viscous material (non-Newtonian fluid) which makes the dynamics more complex. For a Newtonian fluid, viscous forces are proportional to the velocity gradient :

$$\tau = \eta\dot{\gamma} \tag{1}$$

where τ is the tangential stress, η the dynamic viscosity and $\dot{\gamma} = \frac{\partial v}{\partial n}$ the velocity gradient in the normal direction (shear rate).
For a a viscous fluid such our case, the equation 1 becomes the following :

$$\tau = \eta(\dot{\gamma})\dot{\gamma} \tag{2}$$

The ice viscosity is often described as a Glen's flow law which described a strain rate proportional to the tangential stress at a power n :

$$\dot{\epsilon} = A\tau^n \tag{3}$$

with $\dot{\epsilon}$ the strain rate, A the rate factor in $Mpa^{-3}a^{-1}$, τ the effective tangential stress at a power n taken at $n = 3$ in this study as commonly prescribed in ice-flow models ([15]; [4]).

Elmer-FEM is able to run steady as well as transient simulation with time dependence. Both will used in the present study, depend on the problem to be solved. Steady simulation is used for the calibration of the slip coefficient (section 4.3.2) while a transient simulation is used for a prognostic/diagnostic run (section 5.3).
As a boundary condition, a sliding law is used which is discussed in section 4.3.

More recently, a parallel computation has been implemented in Elmer-FEM, a key component for a fast and accurate model.We discussed about the mesh size in the section 4.

3 Area of study

3.1 Storglaciären

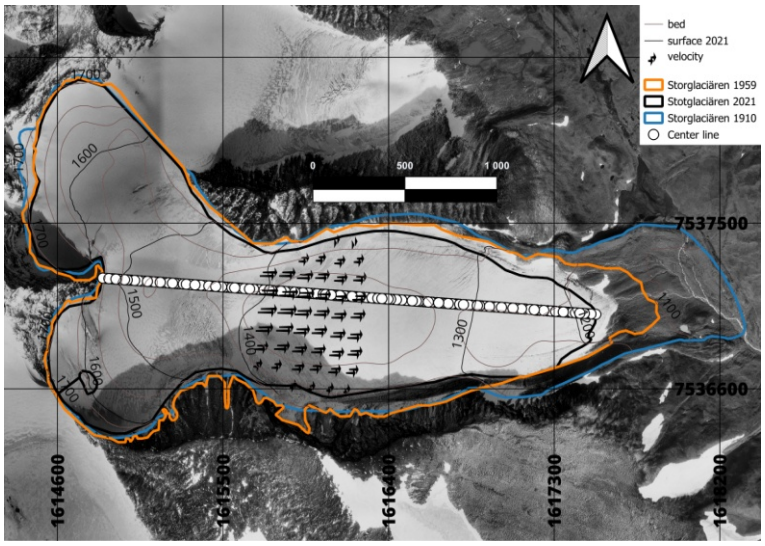

Figure 2: Aerial view of Storglaciären with the shape of the glacier at differnt times and location of data available.

Storglaciären (67.90° N, 18.60° E, 2.77 km² in 2021) is a glacier extended from his head at 1 700 m a.s.l to his terminus at 1 180 m a.s.l. It is temperate on the major part, which mean that the temperature on the ice is close to the melting point and the water content is non-zero. Nevertheless, there is also a cold layer in the ablation area of the glacier.
As a Scandinavian glacier, Storglaciären is characterized by 2 distinct seasons : a cold glaciated winter and an unglaciated summer with a mean seasonal air temperature respectively of -6.6 $\pm 1.1°C$ and 5.9 $\pm$ 1.2$°C$ (BolinC). The seasonal transition takes place during the month of June which can be either a summer month or winter month.
The winter mass balance is carried out at the begining of the spring season in march (which correspond to the winter glaciological season).

3.2 DEM and bed reconstruction

A proper Digital Elevation Model DEM is essential for the model considering it is the input data to deduce the ice thickness. For transient simulation, the DEMs at different time-steps are useful to reproduce the retreat/expansion of the glacier.
Holmlund (data unpublished) made several DEM in order to study the past evolution of the glacier and more recently to have a high resolution DEMs. Thus, surface elevation are available in 1910, 1946, 1959, 1980, 2008, 2015, 2018 and 2021 in different quality.
In addition, Koblet et al.[9] made a re-analysis of aerial images and published DEMs of 1959, 1969, 1980 and 1999. The surface cover by the glacier is well described whereas there is an important uncertainty on the surface elevation.
For the bed reconstruction, Björnsson [3] made a maps of the sub-glacial topography by Ground Penetrating Radar (GPR) in spring 1979 at a high resolution. Some corrections were made using the 2021 DEM.

3.3 Velocity

Ice velocity of a glacier is essential to understand and simulate the flow even though it is tiny compare to water flow for example. To obtain velocity data, high-precision GPS equipment is needed. That is the reason why only few data are available for our area of study. In addition,

modern technology such as remote sensing do not apply in Storglaciären because of its small area.

A grid of surface velocity calculated at the interface between temperate and cold layer was made by Petterson et al.[17], given a mean year surface velocity between May 2001 and May 2002. The resolution is 20 m x 20 m with values interpolated from 46 stakes measured in a 100 m x 100 m grid approximately. The accuracy on measurements is $\pm 5cm$ in horizontal direction. A zero velocity hypothesis at the margins was done for the interpolation. The norm of velocity is given and by definition should be positive. However, there are some negative inconsistent values. Thus, data are filtering and negative values are removed.
Hooke et al.[8] have previously made a records of surface velocity during 3 years between June 1982 and July 1985 given both vertical and horizontal velocity. 23 stakes distributed in both ablation and accumulation area were frequently recorded (7-10d during summer season and 45-90d during winter season). These data give velocity on area not cover by the previous dataset. Unfortunately, data are unpublished and not available. Thus, only qualitative analysis can be carried out.

3.4 Mass balance

A mass balance is crucial in glaciology to estimate the lose/gain of mass by a glacier over the time. 3 terms are key to understanding the process :

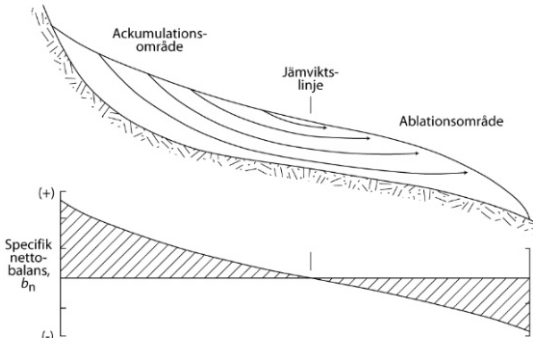

Figure 3: 2D representation of the mass balance along a low line following a glacier ©Peter Jansson

- accumulation area is the part of the glacier where there is more snowfall than melting ;
- ablation area is the part of the glacier where there is more melting than snowfall ;
- Equilibrium Line Altitude (ELA) is the fictive line between both previous parts, meaning that the net balance is zero.

The measurement of the yearly glacier evolution (the net balance B_a) is carrying out by subtracting the summer balance (melting recover during summer B_s) to the winter balance (accumulation occurring in winter B_w). Thus, the annual net balance is compute as the following:

$$B_a = B_w - B_s$$

It means that measurements are done twice a year in the glacier. It is done with traditional stake measurements which consists to compute the relative change at a stakes on the ground. Then, values are interpolated between stakes.
The winter mass balance has been measured in a 100m x 100m square grid which allows a high resolution. Due to the melting in summer, the access is more tricky and summer balance is measured with around 40/50 stakes in the whole glacier which represents a grid around 350x350 m in average. However, due to field condition, it is not possible to get a perfect space grid.
Yearly winter balance, summer balance, net balance and the ELA are published in the BolinC database for each computed elevation band in the period 1946 - 2011. In addition, an overview

of annual mass balance is published until 2015.
The World Glacier Monitoring Service (WGMS) database has an overview of mean winter, summer and net balance since 1946 and the detailed annual mass balance are published since 1981.

4 Methodology

4.1 Mesh

After sensitivity tests, the best possible compromise for a reasonable computing time is a mesh of 40m x 40m at the surface. Due to the small aspect ratio of glaciers, creating a mesh for a glacier geometry cannot generally be done using classical mesh tools.
Here, a structured mesh on a rectangular grid at a given resolution (here 40m x 40m) is created following the dimension of the DEM. To do so, GMSH, a three-dimensional finite element mesh generator is used, keeping the coordinates of the input file. The mesh elements are triangular with 3 nodes (figure 4).
Then, Elmer FEM has his own tool to produce a mesh, which is call ElmerGrid. It is used to transform the previous mesh as a readable mesh for Elmer and initiate the model for the computation. Considering that a parallel computation is done, ElmerGrid is also used to partitioning the mesh, in 20 parts for instance. At this point, we still have a 2D mesh.
In order to get a 3 dimensional mesh, an extrusion is used. A file which contains the bedrock as well as the DEM is input in the model and a solver extruded the previous rectangular mesh in 10 parts evenly distributed on the thickness. It means that if the ice thickness is 200 m, the mesh size in the Z coordinate is 20 m. Also, the file that contains the DEM (or the bedrock) is larger than the glacier. In those parts, $bed = surface$, which means that there is no extrusion.

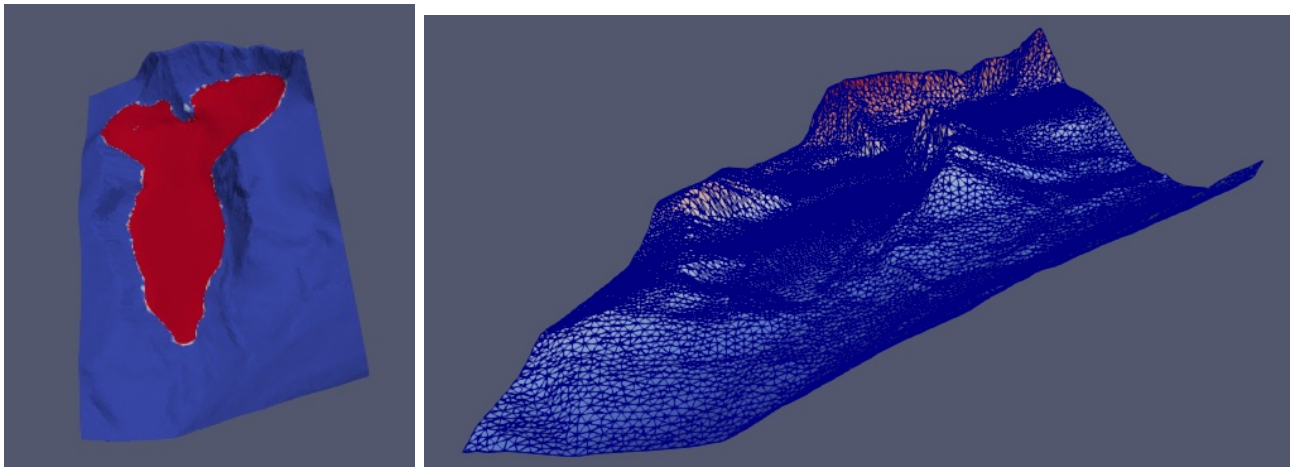

Figure 4: Numerical model of Storglaciären. On the left, the glacier ice surface is represented in red while the ice free surface altitude is in blue. On the right, a representation of the mesh with the surface on the background.

For a transient simulation, the mesh is not updated at each timestep and keep the spatial distribution (same grid coordinates). However, the extrusion is made at each timestep in order to take into account the free surface evolution (increase or decrease in ice thickness).

4.2 Ice rheology

As a viscous material, the ice has a complex rheology. Thanks to the various study on Storglaciären, enough information are available to avoid a numerical calibration.

Density

The density changes over the time, from fresh snow with a low density (around 200 kg/m^3) to pure ice with high density (917 kg/m^3).
Some density measurements has been done in Storglaciären close to the surface. The density profile on a glacier is usually gradual at the first meters of thickness (fresh snow which become ice) and then reach a quasi-constant value. Considering that the variations are only at the top layer (9 m to reach constant value over 300 m of thickness), a constant density is supposed in the whole domain.
We assume a density of 800 kg/m^3 which is an average between the low density in the temperate layer and the high density in the cold layer. Several values has been tested between $\rho = 600\ kg/m^3$ and $\rho = 917\ kg/m^3$.

Rate factor

The rate factor is the viscosity parameter on the Glen's flow law. It is sensitive to temperature and several other parameters such as pressure, impurities in the ice and crystal (size, shape and orientation). Thus, it is a parameter which it changes in space and time but usually, an average is taken into account in the model. For ice sheet modelling at a large scale or without ice rheology information, there are some classic values. For the present glacier, a calibration has been done by Albrecht et al.[2]. Hence, the value of this calibration is used : $A = 9Mpa^{-3}a^{-1}$, which is close to other poly-thermal glacier and according to Patterson 2010[14], it corresponds to ice at a temperature of around $-6.5°C$. In addition, vertical temperature profile has been done in the valley, showing an average temperature of around $-3°C$ between 0 and 100 m depth (intern communication).

4.3 Sliding

As we have seen in section 3, data are available in the surface (apart the bedrock deduced by radar). However, basal behaviour is a key for the numerical simulation. A better understanding of the sliding of glaciers / Ice sheets is one of the challenges of numerical modelling.

4.3.1 Sliding laws

Several friction laws has been developed for glaciology and depend mainly of the glacier termination, slope and topography. It can also be effective-pressure dependant, assuming knowledge of this pressure, which is not usually the case for glaciers.
On the other hand, Elmer-Ice has several friction laws and we will focus on glacier friction law. The most basic one is a linear friction law, related the basal velocity to the basal shear stress with a linear coefficient C such as :

$$\tau_b = Cu_b \tag{4}$$

with τ_b the basal shear stress, C the slip coefficient and u_b the sliding velocity.
This linear sliding is only slope dependant. It is well adapted for the following case :

- slow velocity;
- simple topography or absence of bedrock data;
- numerical issues which not allow to implement a complex law (cost and time computation).

Storglaciären has a slow velocity. However, there is a good knowledge of the topography and the small area of the glacier allow to take into account a complex law. That is why a non-linear law is introduce in the model. It is a Weertman friction law[18], and the basal shear stress is expressed at the following :

$$\tau_b = C u_b^{m-1} u_b \tag{5}$$

C is the Weertman friction coefficient, m the Weertman exponent. m is defined as $m = 1/n$ or $m = 1/3$ in our case with $n = 3$ defined in 2.2. The law is linearized for very small velocity and the parameter to calibrate is C (see section 4.3.2).

The cavitation is a key of sub-glacial behaviour, especially for temperate glacier such as Storglaciären. Nevertheless, this phenomena is not easily simulated and not taken into account in the 2 precedents law. Thanks to Gagliardini et al.[7], a water-pressure dependant non-linear friction law has been developed (see B and the paper for additional information). It is a regularised Coulomb law available in Elmer-Ice. 3 parameters have to determined to implement this law :

- A_s which relates the basal shear stress and the sliding velocity before cavitation. It can be estimate from FEM simulation assuming that the ice rhelogy and the bedrock are known.
- C is a constant for a given bedrock geometry, independant of Glen's flow exponent.
- q controls the post peak decrease of the friction law. The value is related to the shape of the bedrock (saw-tooth, ellipsoidal or sinusoidal bedrock).

The water-pressure dependence is the first limitation of this law considering it is not well known in Storglaciären. Then, it is not implemented for an inverse method (see section 4.3.2).
Thus, the chosen methodology is to use first a Weertman friction law for the calibration of the slip coefficient and switch to a Coulomb regularized law with some assumptions (see details in B).

4.3.2 Inversion

The inverse methods are used in glaciology in order to determine largely undetermined parameters such as basal friction. To do so, surface data is needed in order to calibrate the parameter. The surface velocity data described in section 3.3 are used to make the inversion. A simulation is ran with a define basal friction (here a Weertman friction law). Then, the surface velocities are exported and compared to the data. The difference between both is called the discrete cost function J. Considering the data are expressed as a norm velocity, the cost function is expressed such as :

$$J = \sum_{1}^{Nobs} 0.5 ||(u - u^{obs})/std||^2 \tag{6}$$

where N_{obs} is the sum of the number of observation, u the modelled surface velocity, u_{obs} the observed surface velocity and std the standard deviation.

In absence of information about the error on measurements, an uniform standard deviation is applied on the measurements :

$$std = \sqrt{\frac{1}{N_{obs}} \sum_{1}^{Nobs} (u_i^{obs} - \mu)^2} \tag{7}$$

with μ the mean of the observations.
The aim of the inverse method is to minimise the cost function. Here are the steps description of the method:

1. Compute the velocity using the Stokes solver;
2. Compute a cost function that measures the difference between the model and some observations;
3. Compute the solution of the adjoint linear system;
4. Compute the gradient of the cost function with respect to the slip coefficient;

We are looking to minimise the gradient in order to converge toward the smoothest solution. To do so, a quasi-Newton algorithm is used (see [11] for more information).
In addition, the problem is ill-posed and it does not exist a unique solution. That is why a regularisation is added in order to approach the 'true minimiser'. To do so, the variation of the derivative of the cost function with respect to variation of the calibrated variable (here the basal friction parameter) should be minimum:

$$Grad(J') = \frac{\partial J}{\partial \beta} = 0$$

In Elmer-Ice, a classic regularisation is implemented, which penalises the first spatial derivative (equation 8) or use a prior(equation 9). In other words, the regularisation will insure a smooth variation of the slip coefficient in space or insure that the slip coefficient is close to an initial guess.

$$J_{reg} = \int 0.5 |\frac{\partial C_{opt}}{\partial x}|^2 d\Omega. \tag{8}$$

$$J_{reg} = \int 0.5 (\frac{C_{opt} - C^{mean}}{s^2})^2 d\Omega. \tag{9}$$

with J_{reg} the regularisation term, C_{opt} the optimised friction coefficient, C^{mean} the initial guess (prior estimate) and s^2 the variance over the surface domain Ω.
So far, the regularisation was only possible on the whole domain of study. We have seen previously that the observed velocity data are only available on a small part of the domain (section 3.3). Thus, a new method was implemented in Elmer during the present study and used as a test case (see Recinos et al.[10] for methodology).
Here, the regularisation term is defined as follow :

$$J_{reg} = \int 0.5 || \frac{C_{opt} - C^{mean}}{B} ||^2 d\Omega. \tag{10}$$

Where B is a correlation matrix defining the trust on the prior. It is a Matérn type covariance matrix which is function of the space (e.g the covariance between 2 points depends of the distance between this 2 points). 3 parameters have to be defined :

- *nu* is an exponent of correlation function and controlling the smoothness of the learned function by defining the correlation type at a short distance. We set it at 1 in the model and will not change it.
- *range* is the auto-covariance length scale (in m.) defined the length scale of the kernel : in which distance friction coefficient values are correlated. The parameter has to be calibrate.
- *std* the standard deviation of the auto-covariance length scale (same unity as friction coefficient) defined the variability of the friction coefficient for long-range values.

The covariance length scale is described to be around 1 and 20 times the mean ice thickness for big ice sheet fast flowing according to De Rydt et al.[6] whereas it is defined less than about 5 and 10 times the mean ice thickness for ice shelf according to Gudmundsson[12]. Both of these order of magnitude are given for big ice sheet/ice shelf with smaller variations in space than alpine glaciers. Here, we defined the covariance length scale at the mean ice thickness (i.e 55 m) as well as Recinos et al.[10].
For the standard deviation, it does not exist empirical relation as well as order of magnitude in literature. Thus, this parameter will be subject to a calibration in section 5.1.2.

4.4 Mass balance gradient

The surface evolution over the time is reconstructed by the implementation of recorded mass balance as a function of elevation. To do so, a mass balance gradient db/dz is computed in both ablation and accumulation area for each yearly mass balance record and implemented in the model. The gradient reproduces the yearly balance (net balance B_a) variation with altitude from the ELA to the top/bottom of the glacier.
This implementation of mass balance gradient do not taken into account temperature data and precipitation data. It means that for a future simulation, a correlation must be find between climate data and mass balance gradient.

4.4.1 Gradient computation

Mass balance data are given by band of elevation with the net balance for each band. Two methods are defined to compute the gradient :

$$db/dz \;=\; \frac{B_0}{Z_0 - ELA} * 100 \quad (in\ \frac{m.w.e}{100\ m}) \quad \textbf{Diff method} \tag{11}$$

where B_0 is the net balance at the bottom/head of the glacier for respectively ablation/accumulation gradients with a corresponding altitude Z_0.

$$db/dz \;=\; \frac{1}{N} * \sum_{n=1}^{N} (\frac{B_n}{Z_n - ELA}) * 100 \quad (in\ \frac{m.w.e}{100\ m}) \quad \textbf{Mean method} \tag{12}$$

where B_n is the net balance corresponding to the band n for the lower bound or upper bound for respectively ablation and accumulation gradients at the altitude Z_n, whereas N is the number of band.
Due to inconsistent data such as positive net balance at the bottom of the glacier, equation (11) gives some incorrect data at some year. Then, the ELA is not always consistent with the given data. Indeed, net balance can be positive/negative until an altitude below/above the

ELA. To avoid additionally bias, inconsistent values mentioned above were filtered.
Two dataset are available (see section 5.2). The noticed inconsistencies were in the data availbale at BolinC. Thus, data provided from WGMS have been promoted. BolinC data were used from 1946 to 1980 (apart for 1960 and 1963 when no data were published) because it is the only available whereas between 1981 and 2019, WGMS data were used. An exception in 1990 is made because a maximum accumulation of around 16 m is given with WGMS data. Then, in 2004 and 2005, ELA is not given, so ELA from BolinC data is taken.
A linear relation between is assumed in both methods, which is usually the case for alpine glaciers with a curvature observed at the margins[1]. Both methods are compared with a classic coefficient of determination r^2 computed for each year.
In addition, between 2004 and 2011, BolinC database provide a mass balance gradient in ablation area with the same assumption of linear relation with altitude. Unfortunately, there is no method description attached to the data.

4.4.2 Gradient polynomial regression

As a small glacier, Storglaciären has a small range of elevation between the bottom/head of the glacier and the ELA. Thus, the curvature mentioned above (section 4.4.1) can have a strong effect. A polynomial regression using a statistical analysis is done in order to see the effects of adding non-linear-terms.
First, a linear regression is assumed to compare with the previous linear methods. The intercept is already known (e.g ELA) and only the slope is determined in function of the surface elevation $Z_s \pm ELA$. Then, the coefficient of determination is computed Using scikit-learn[16] library in python. The residual sum of squares between oberved mass balances and predicted mass balances by the linear approximation is minimised :

$$\min_{\frac{db}{dz}} ||Z\frac{db}{dz} - B_a||_2^2 \tag{13}$$

where Z is the corrected elevation, $\frac{db}{dz}$ is the mass balance gradient and B_a the recorded net annual mass balance.

Then, a polynomial regression is also tested to considering non-linear features of the balance function. Here, a pure polynomial feature is used. It generates all the monomials up to a given degree (in the present study, degree 2 and 3 are tested).
For a degree defined at 2 and 1D a dataset of Z_s given the surface altitude, the polynomial features do the following computation :

$$\begin{bmatrix} Z_{s1} \\ Z_{s2} \\ ... \\ Z_{sn} \end{bmatrix} => \begin{bmatrix} Z_{s1}^1 & Z_{s1}^2 \\ Z_{s2}^1 & Z_{s2}^2 \\ ... & \\ Z_{sn}^1 & Z_{sn}^2 \end{bmatrix} \tag{14}$$

Then, a linear regression is done using multiple variable (2 for the previous example).

4.5 Numerical resolution

One of the biggest challenge of FEM is to get a convergence of the system. The Stokes solver, solved the Stokes equations described in section 2.2 and the numerical parameters are essentials to converge on the right solution. A linear Stokes system is solved at each non-linear iteration needed to the non-linear rheology (e.g Glen's law in section 2.2).
There are 2 distinct methods for the linear system in FEM:

- Direct solver
- Iterative solver

The direct solver is easier to implement and to avoid numerical issues up to 100 000 unknown in the system. Thus, for big computationally problem, the iterative method can be useful. However, the second solution gradually move towards the correct solution and it needs a preconditionner to well constrain the problem and initialise the initial guess (see [5] to the method tested).
For the present, when the problem getting complex, none preconditionner was find which satisfied a convergence of the system. Thus, the direct method was used and the mesh size slightly increased if numerical issues appeared because of the number of unknowns. MUltifrontal Massively Parallel Sparse direct Solver (MUMPS) is the parallel direct solver used for the linear system.

The non-linear system, is already implemented in Elmer-Ice. Two methods can be used :

- Picard fixed point iteration
- Newton linearisation iteration

The Newton linearisation is much faster and converge toward a solution in less iteration whereas the Picard fixed-point is more stable. There is no rules and the method can be adapted at each simulation.
The general case for the present is to use a Picard iteartion until a convergence of 10^{-03} and then switch to Newton iteration. In some cases, only Picard iteration has been used involving a longer computation time. The total convergence tolerance is fixed à 10^{-08} for all the simulations.

5 Results

The results obtained during the study are dependant from a simulation step to an other. Indeed, the inversion has been ran first with a steady model (no time dependency) and from this inversion, a transient simulation can be calibrate with the defined slip coefficient.

5.1 Inversion

The inversion is made using a steady state simulation and the DEM from 2021 is used as surface elevation reference to get the best accuracy possible.

5.1.1 Prior

In the absence of surface velocity data which cover the whole domain, a prior (initial guess of the slip coefficient) is used for the regularisation term (section 4.3.2). To find the prior, several simulations are run using a Weertman friction law with and changing the friction coefficient value (which is uniform over the whole domain for each simulation).
The range of value tested is from $C = 1$ to $C = 0.001$ which simulate a maximum velocity from 3 m/yr to more than 200 m/yr. Then, a finer increment was implemented between $C = 0.02$ and $C = 0.035$, with a qualitative comparison of surface velocity available. The final value for the prior is a coefficient $C = 0.0275$.

5.1.2 Standard deviation

The standard deviation (std) is tested for a range scale from $std = 10^{-04}$ to $std = 10^{-01}$. Under $std = 10^{-04}$, there are no change in terms of slip coefficient whereas above $std = 10^{-01}$, too high values of velocity are observed.

Grid calibration

Data from calibration from Petterson et al.[17] were made with an interpolation (see section 3.3 for details). Using this grid and by altering *std* parameter in the range given previously, an inversion is made.
The zero velocity at the margins is a strong hypothesis considering that the stakes close to the margins give a velocity around 5 $m/year$ and the maximum velocity in the middle of the grid is around 20 $m/year$. Thus, the inversion gives a really high slip coefficient only on these parts, which is very different from the rest of the glacier (figure 5 A). In addition, the velocity simulated diverges from the grid at these parts and there is a big area where the simulated can not converge to the right value (figure 5 B).

Stakes calibration

To overcome the previous problem, draw velocity data (without interpolation) were used in order to reduce uncertainty even if the cover area is reduced.
Results of the inversion in function of the value of *std* are shown in table 7. Logically, the RMS increases with std because the slip coefficient is less constrain. The order of magnitude of the

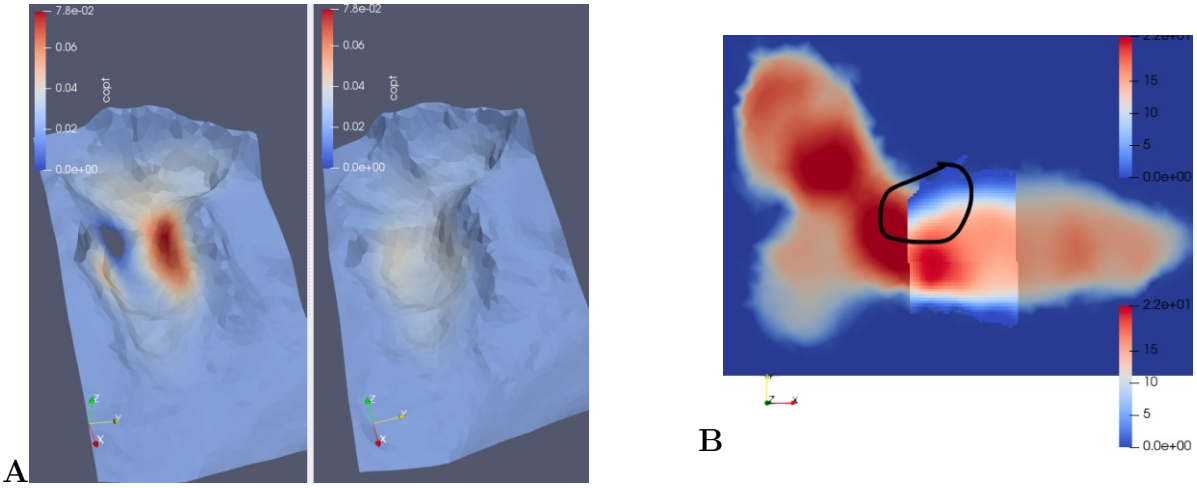

Figure 5: A) Slip coefficient deduced from the inversion, first with the grid interpolated of velocity and then with draw velocity. B) Map of simulated velocity in the whole glacier (background colormap) and grid of velocity made by Petterson et al. on the foreground. Both velocity are expressed in $m/year$. The area circled by the black marker shows the big difference between both models. The simulated velocity is computed at a resolution of 40m square and interpolated using bi-linear interpolation whereas the grid interpolated of velocity is plotted at a resolution of 20m square.

maximum surface velocity is close to the maximum observed. Considering that the maximum velocity is out of the area with observation, it means that the model is able to well reproduce the basal sliding in the whole domain.

std	**RMS [m/yr]**	**us$_{max}$ [m/yr]**	**uv$_{max}$ [m/yr]**	**Copt$_{mean}$**
$\mathbf{1.10^{-04}}$	4.91	20.532	3.806	0.0275
$\mathbf{1.10^{-03}}$	4.86	20.628	3.832	0.0274
$\mathbf{5.10^{-03}}$	4.03	22.473	4.319	0.0265
$\mathbf{1.10^{-02}}$	3.30	24.750	4.811	0.0255
$\mathbf{5.10^{-02}}$	1.45	31.949	5.006	0.0246
$\mathbf{1.10^{-01}}$	1.04	33.722	5.094	0.0246
$\mathbf{1.10^{-04}}$	0.652	36.184	6.230	0.0259

Table 1: Results of simulations using a different value of standard deviation (std). The Root Mean Square (RMS) designates the mean absolute difference between surface velocity simulated and surface velocity observed whereas us_{max} and uv_{max} designate respectively the maximum horizontal and vertical surface velocity simulated. $Copt_{mean}$ is the mean value of friction coefficient optimised at the the end of the inversion in the whole domain.

Figure 6 shows the repatriation of the slip coefficient for each inversion. For a small value of *std*, the slip coefficient is uniform and almost equal to the initial guess. When *std* increases, the model converge to a higher value of C_{opt} where observations are available as we have observed with the inversion using the grid.
A qualitative analysis (figure 7) has been done to compare the values in the other area where velocity is available. The maximum surface velocity (horizontal and vertical) given by the inversion was compared to the maximum observed by Hooke et al.[8]. Horizontal velocity has been favoured considering there are less uncertainty on the values. Thus, calibration was selected with $std = 5e-03$ which in addition allows a higher variation of the coefficient to simulate the difference in basal behaviour out of the observed data (different rheology and slope).

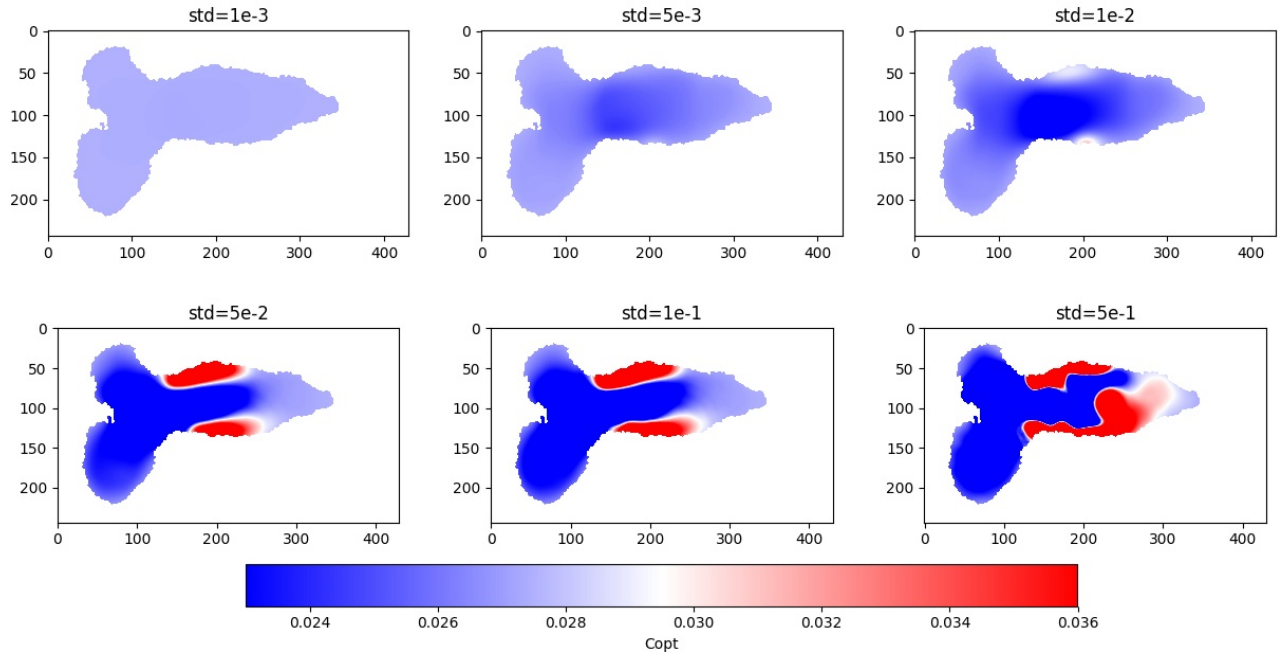

Figure 6: Plot of error between observed/modelled maximal velocity and RMS in function of the value of std. The error is expressed in absolute value whereas the maximal observed values taken into account are respectively 21 m/y and 7 m/y for horizontal and vertical velocities according to Hooke et al.[8]. The dashed line highlights the chosen value of std. Value of x and y are given in pixels and one pixel is 10 m x 10 m square.

5.2 Mass balance

The relation between mass balance variation in function of elevation is sought in this section. A linear relation can be a good approximation for alpine glaciers with usually a non-linear behaviour at the margins[1]. However, Storglaciären has a small range elevation, which can restrict the linear relation. Moreover, melting and accumulation are much more influenced by the season than the altitude for high latitude glaciers. Indeed, there is almost no freezing in summer whereas the entire glacier is is subjected to temperatures below zero the winter, which can drive to a constant melting/accumulation at different altitude ranges. Finally, a part of the glacier is subject to strong avalanche deposits due to the steep slopes around which can once again driven to a non-linear relationship.

5.2.1 Gradient computation

The variation of the mass balance distribution over the year, did not allow us to define a better method. We could just select the better fit with the higher r^2 but each method have some years when the mass balance is very poorly reproduced. Figure 8 illustrates this phenomena. Thus, it is worth to combine both methods and select for each year the one which have the higher determination coefficient. Moreover, considering the gradient is computed in ablation and accumulation area, we select the best fit in both area (the two methods can be used for one year).

The mean method has a better ability to reproduce the parabolic behaviour of the mass

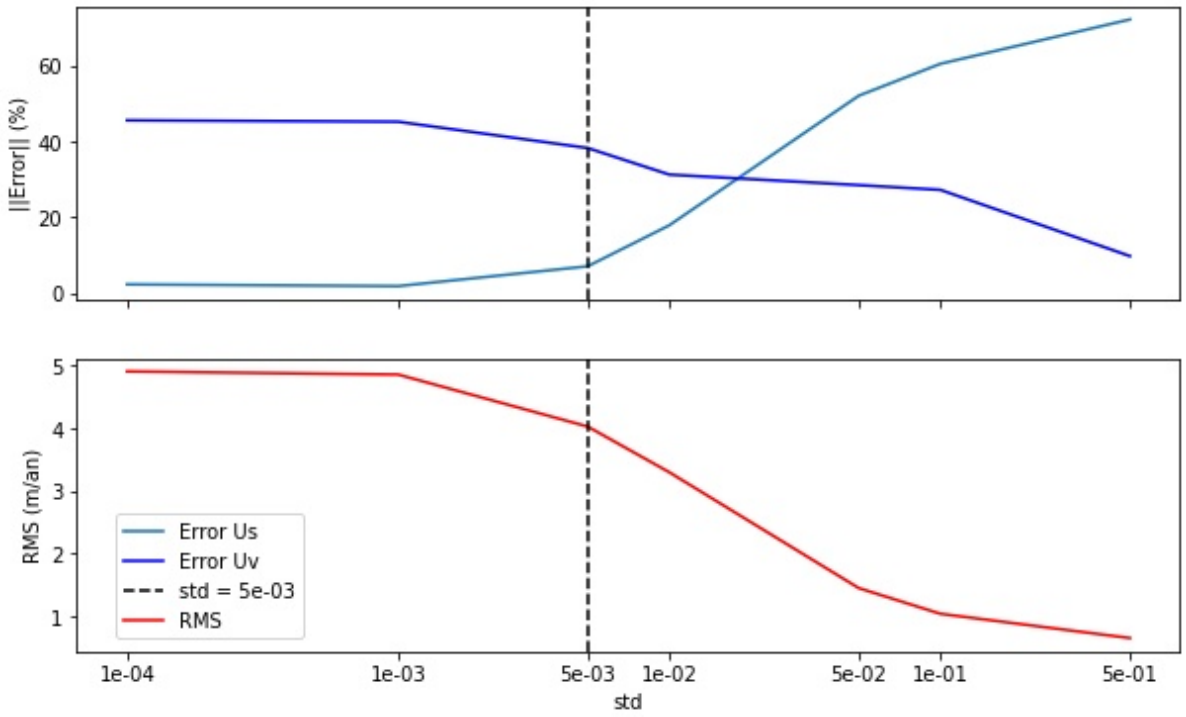

Figure 7: Plot of error between observed/modelled maximal velocity and RMS in function of the value of std in log scale. The error is expressed in absolute value whereas the maximal observed values taken into account are respectively 21 m/y and 7 m/y for horizontal and vertical velocities according to Hooke et al. (cite 3 years velocity). The dashed line highlights the chosen value of std.

balance distribution at the margins whereas the difference method is mainly used when we observed a sinusoidal relation.
The accumulation area has a better linear behaviour and the correlation is higher ($r^2_{accu} = 0.76$ in average). Here, the difference method gives 42 better correlation over 58.
It is complex to defined a general tendency in ablation area and the determination coefficient is lower ($r^2_{abla} = 0.59$ in average). Nevertheless, the mean method seems better considering the variations are important with the altitude. Indeed, over 58 time-steps, 51 gives a better correlation with the mean method. Between 2004 and 2011 we have compared the gradient already computed in BolinC and computed the coefficient of determination (figure 8 D). For this short period, we got a coefficient of determination $r^2_{abla} = 0.52$ whereas in the same period, the mean method gives $r^2_{abla} = 0.70$. Only the year 2007 gives a better r^2_{abla} and the error is only reduce by 2% on that period.
Also, with the time, the ELA tend to be higher as well as the bottom of the glacier (glacier retreat). The non-linear behaviour of the ablation mass balance distribution is mainly observed at the very bottom of the glacier. Thus, by comparing the determination coefficient during 1959-1992 and 1993-2019, we observed an important difference. Indeed, in the first period $r^2_{abla} = 0.51$ compared to $r^2_{abla} = 0.70$ in the second period. This fact is related to the necessity of a wide elevation range to get a strong linear relationship.
This difficulty to establish a clear relation deserves a closer look to be able to produce a consistent mass balance in the numerical model in function of future climate scenarios.

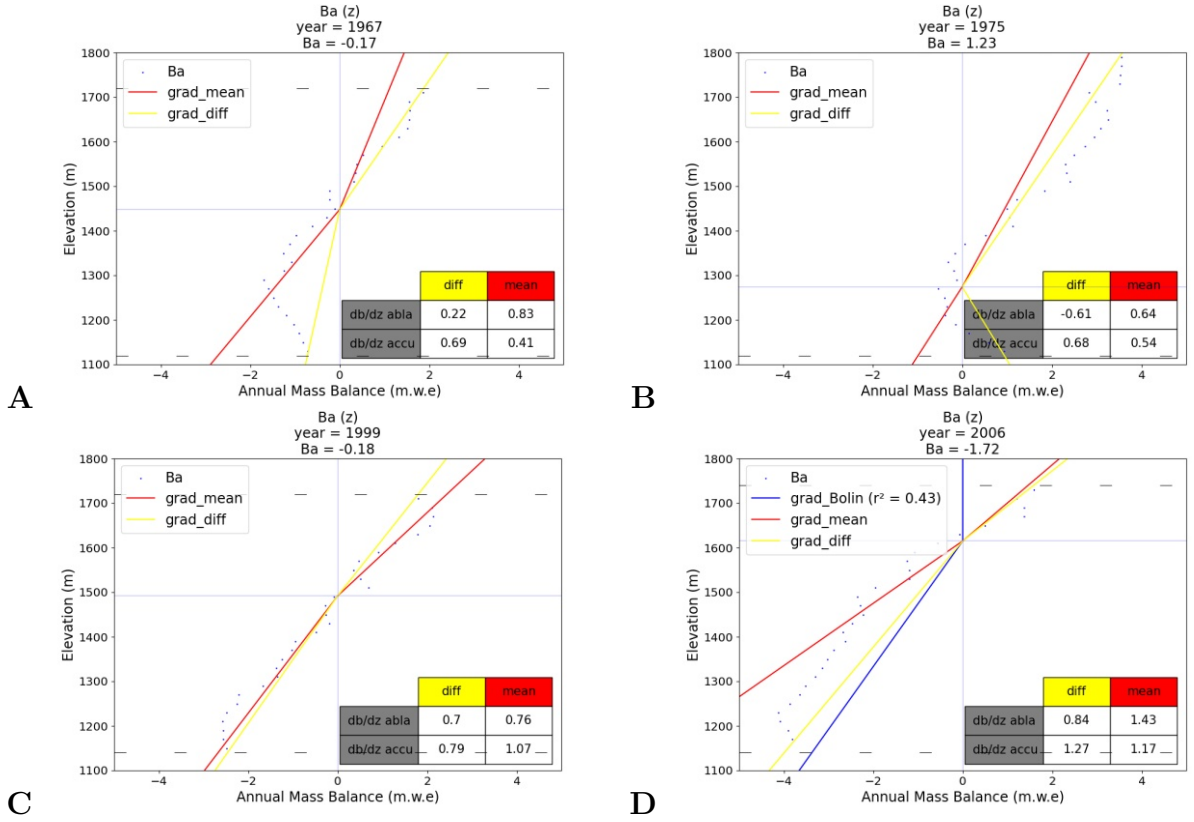

Figure 8: Several plots of annual mass balance computed with gradient using difference (yellow line) and mean method (red line). Blue dot points represent the annual mass balance measured on site with both head ans bottom limits of the glacier represented by black dashed lines. The ELA is represented by the horizontal blue line whereas the vertical blue line shows the zero balance. From the upper left to the lower right: A) case where the ablation has a complex shape better simulated by the mean method whereas the accumulation is pretty linear and better simulated by diff method B) case with an ELA really low (year with glacier expansion) showing the complexity to find a relation between mass balance and elevation C) case with a linear behaviour of a distribution and a high correlation with the mean method D) case with the ablation gradient available in BolinC (blue line).

5.2.2 Gradient polynomial regression

Here, we focus on the linear regression to see if a better representation of mass balance function of altitude can be figure out and implemented in numerical model. First, a linear regression has been made and compare to the previous linear models whereas in a second step, a polynomial regression to the second and third order have been tested.

Linear regression

The linear regression with a first order allows to improve some correlations, but mainly when the distribution is linear. Thus, the problem highlighted previously is not solved. Indeed, there are 20 years when the regression gives a negative r^2_{abla} value, meaning that it is more efficient to predict directly the mean value.
Among the 58 time-steps, 18 of them can get a better coefficient of determination using the linear regression and if we focus on these 18 time-steps, the average coefficient is $r^2_{abla} = 0.77$ against $r^2_{abla} = 0.62$ using the better value with the two methods of computation described previously.
From a general perspective, if we look at all the time-steps, the gain using the linear regression is only 2% (from $r^2_{abla} = 0.59$ to $r^2_{abla} = 0.61$).

In accumulation area, the linear regression gives pretty much the same results than with the gradients computed. It confirms the linear tendency of this area.
In brief, the first order linear regression allows to improve the mass balance distribution at some points. However, it is even worst than the previous methods to reproduce the complex distributions. Once again, this method can be a good way of combining.

Second and third order regression

We investigate here the ability of a polynomial regression to reproduce the mass balance distribution. Due to the parabolic curvature of the ablation area (and more generally at the margins), the second order seems a good way. In addition, the third order is also tested to visualised the effect of it in the predict mass balance.
First of all, the addition of a non-linear term avoids the negative r^2 mentioned in the previous section. Indeed, the second and third order have only one negative value of r^2 both in 1965 and this value is associated to the distribution of the mass balance which is almost constant in the ablation area (see figure 9 A).
Here, we split the results in two dataset :

- Years when the value of linear regression is higher to the mean value ($R^1_{year} > mean(R^1)$) ==> linear behaviour.
- Years when the value of linear regression is higher to the mean value ($R^1_{year} < mean(R^1)$) ==> non-linear behaviour.

Where R^1_{year} represents the yearly coefficient of determination obtained by linear regression and $mean(R^1)$ is the mean over the whole period studied without negative determination coefficient ($R^1 < 0$).
As it has been shown previously, in the first dataset, the first order regression (linear regression) has a good ability to reproduce the linear behaviour with a determination coefficients of respectively $r^2_{abla} = 0.81$ and $r^2_{accu} = 0.89$. Thus, the second and third order does not improve anymore the determination coefficient (around +2%). On the other hand, significant changes are observed in the second dataset and the non-linear behaviour is much better reproduced. In that part, the determination coefficient obtained by linear regression is really low ($r^2_{abla} = 0.81$ and $r^2_{accu} = 0.63$). The polynomial regression reduces the error up to 64% and 24% in respectively ablation and accumulation area (see table 2 for details).

Figure 9 shows the mass balance distribution with the first, second and third order regression. The second order has a shape which well fits with the observed mass balances, in particular for the curvature mentioned above whereas the third order add a new term improving mathematical correlation but making less physical sense for the addition of a generalised function (figure 9 B).
In terms of results, with the polynomial regression, we got the same determination coefficient in ablation and accumulation area (difference of ± 0.01). The third order reduce the error of 4% in relation to the second order.

5.3 Transient simulation

Here, we try to reproduce the evolution of the glacier observed in the period 1959 - 2017 to initialize the model with a good thickness accuracy (DEM in a good quality). We assume

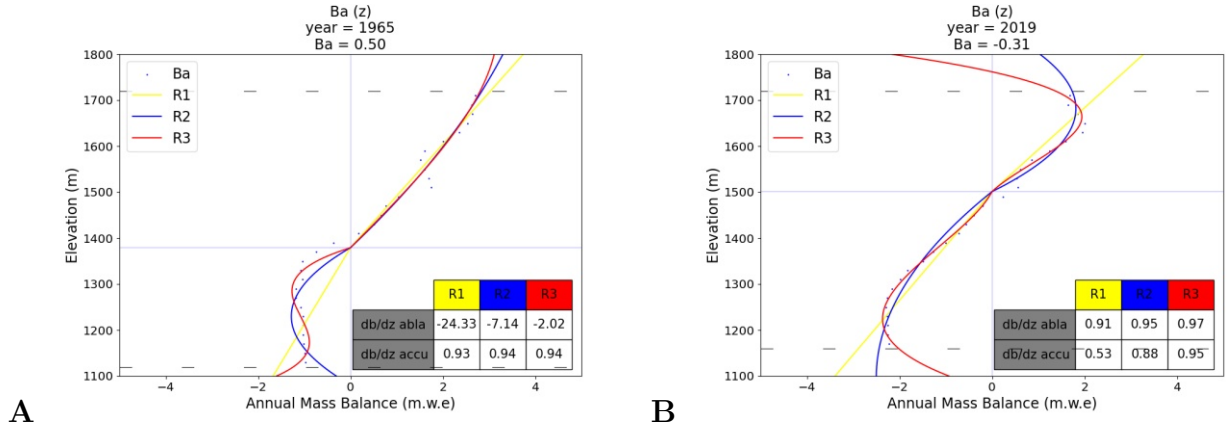

Figure 9: Annual mass balance computed with gradient using polynomial regression from first to third order (respectively R1, R2 and R3). The blue points represent the annual mass balance measured on site with both head ans bottom limits of the glacier represented by black dashed lines. The ELA is represented by the horizontal blue line whereas the vertical blue line shows the zero balance.
From the left to the right: A) case where the ablation has a complex shape and none of the regression succeed to reproduce the distribution B) usual case with improvement of determination coefficient by increasing the polynomial order but a really high curvature can be observed at the margins with the order 3.

	diff	**mean**	$\mathbf{R^1}$	$\mathbf{R^2}$	$\mathbf{R^3}$
$\mathbf{r^2_{abla}}$	0.575	0.235	0.609	0.834	0.876
Missing values	0	4	20	1	1
$\mathbf{r^2_{accu}}$	0.533	0.702	0.803	0.0.844	0.889
Missing values	0	0	3	1	0
$\mathbf{r^2_{mean}}$	**0.554**	**0.469**	**0.706**	**0.839**	**0.883**

Table 2: Mean values of determination coefficient for accumulation area, ablation area and the average of the previous 2 computed for each methods. The negative correlation (e.g $r^2 < 0$) are not taken into account in the mean and are counted in missing values rows.

no change in basal condition over the time and keep the basal surface described in 3.2. The surface change is compared at the different time-steps described in section 3.2. Due to the large error on the surface for the DEMs between 1969 and 2017 (DEM 1969, 1980, 1990, 1999 and 2017) the thickness is not used for comparison. However, proper surface DEMs in 2015 and 2021 exist and are used to know the final volume, maximum thickness, mean thickness and volume change in the whole period. In addition, the yearly mass balances (section 4.4.1) give the volume change and thickness change for each year with stakes interpolation (geodetic method) which are useful to know the ability of the model to reproduce the observations at each time-step. Please, note that the yearly mass balance data are only available from BolinC database until 2012. Thus, 49 time steps are compared.

5.3.1 Numerical issues

Obtain a convergence of the numerical model is very challenging for a parallel simulation using a transient run with 60 time-steps. Different numerical method were tested without success. Thus, the following steps were implemented in the model :

- Mesh size increases from 40 m square to 100 m square.
- Minimum ice thickness increases from 1 to 10m thick to avoid to large expansion of the glacier.

- Adding a maximal slope beyond which accumulation does not occur because of avalanches (avoid non-physical extension of the glacier as well).
- Decrease the computation domain and shape it at the size of the glacier in 1910, meaning that the glacier can not expand out of this domain.
- Decrease the split of the mesh for parallel computation from 20 to 5 (with the smaller computation domain, it does not change anymore the area of each part of the split mesh).

With all these assumptions, a convergence is obtained.

5.3.2 Results

We focus here on 3 models which all have a separate coefficient(s) in ablation and accumulation area :

- Linear mass balance function of altitude implemented with the better linear gradient fitted the observation between the difference method, the mean method and the linear regression (call **optim**).
- Linear mass balance function of altitude implemented with the linear regression made at the first order (call $\mathbf{R^1}$).
- Second order polynomial mass balance function of altitude with the polynomial regression made at the second order (call $\mathbf{R^2}$).

Despite a good fit with observations, the net balance is not always with the same sign between model and observation as well as volume change. The table contain in figure 10 summarises these "inconsistent" values.
The yearly volume change and net balance are poorly simulated with around 1/4 of the time steps which simulates the opposite behaviour (extension simulated for a retreat observed and so on). In addition, the amplitude of the error (RMSE) is larger than the mean annual observation :

$$||\overline{dV}|| = 1.68.10^6 m^{\ 3} \quad and \quad ||\overline{dH}|| = 0.52\ m.w.e$$

(respectively absolute mean annual volume change and thickness change).
On the other hand, if we look at a larger time scale, the retreat of the glacier in terms of surface is well simulated with a small relative error at the end of the simulation. The worst model in terms of volume change gives the best area change.
The Volume change simulated with the "optim" gradient is close to the observed one (only 15% of error in 60 years) and a bit overestimate whereas the linear and polynomial regression underestimate the volume lost, especially the linear regression which predict a small expansion of the glacier ($1.10^6\ m^3$ gained against $50.10^6\ m^3$ lost observed).
Figure 10 helps to understand that the previous findings are explained in the last decades. Indeed, the "optim" model well reproduces the period 1990-2010 whereas the "R2" model has a big expansion in the period 1990-2010. On the same period a constant (or even a small expansion) has been observed. This would shows that the polynomial regression would overestimates the expansion of the glacier. Nevertheless, if we look back to the beginning of the observation (1965-1990), "R2" model has a really good fit with the observed volume of the glacier.
For the following of the study, the so-called "optim" and "R2" method will be studied in depth whereas the "R1" model has a really bad ability to input the observed mass balance.

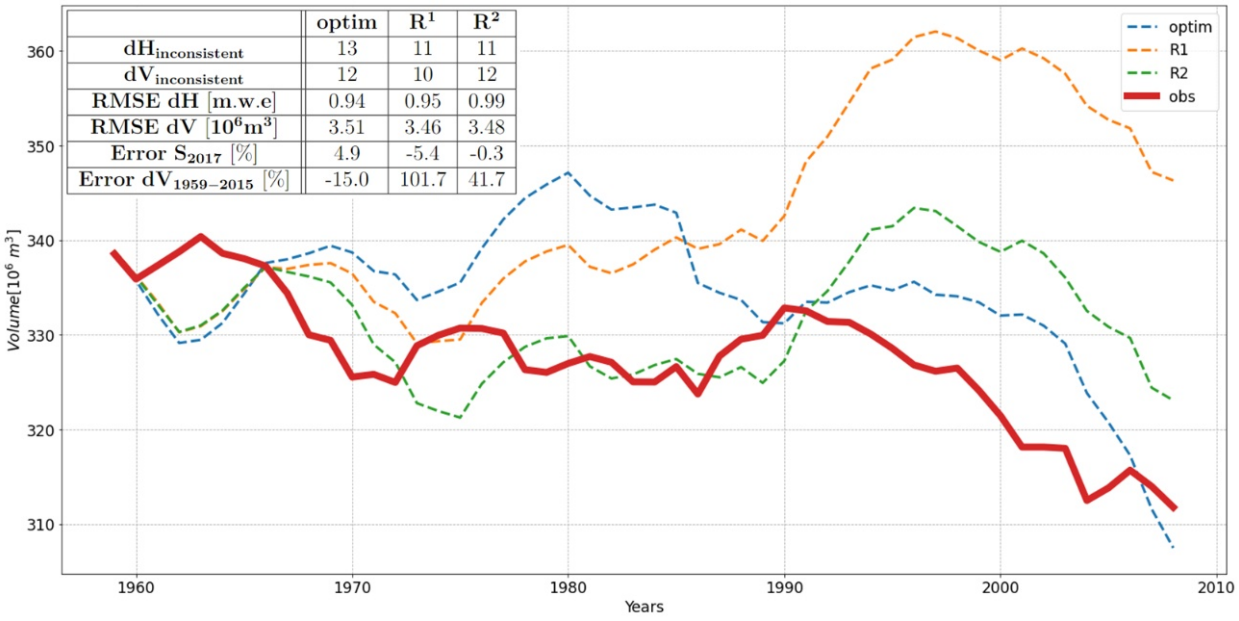

	optim	R^1	R^2
$dH_{inconsistent}$	13	11	11
$dV_{inconsistent}$	12	10	12
RMSE dH [m.w.e]	0.94	0.95	0.99
RMSE dV [$10^6 m^3$]	3.51	3.46	3.48
Error S_{2017} [%]	4.9	-5.4	-0.3
Error $dV_{1959-2015}$ [%]	-15.0	101.7	41.7

Figure 10: Volume in function of year for the 3 models tested. The observed volume change is plotted in red reinforced line. On the corner, table with : a)Number of value with a different sign between observation and model in terms of yearly net balance and volume change. b)Root Mean Square Error of the two previous quantity are computed as well. c) Relative error on the surface at the end of the simulation (2017) and on the volume change at 2015.

It is also essential to check a periodically reproduction of the glacier evolution. Indeed, few behaviours were observed on the glacier since the few decades[13]. A transect in the centre line (figure 2) has been done between different periods to see the difference of surface elevation change (Holmund and Jansson internal report). Unfortunately, it is note available in numeric version. However, it shows a marked diminution of the surface elevation from between 1961 and 1982 with a huge pick at the lower middle and a slight increase at the upper middle. For the period 1982-1995 part of the quasi-stationary state which was observed, the profile is pretty constant. Figure 11 shows the plot on the centre line for the 2 periods. The change in surface elevation is the same than in the transect for both period, showing the ability of this model to reproduce the mass balance in space and time.

Koblet et al.[9] as well as Holmlund et al.[13] are in agreement to describe the glacier evolution with a slowing of the melting from the 50s - 60s to the 80s before a state equilibrium of around 20 years and then a more pronounced return to melting until nowadays. This study confirm this observation (figure 11). The volume change is not in the same magnitude and it remains an important uncertainty since with the polynomial regression (R2 model), gives a pretty different magnitude (figure 12).

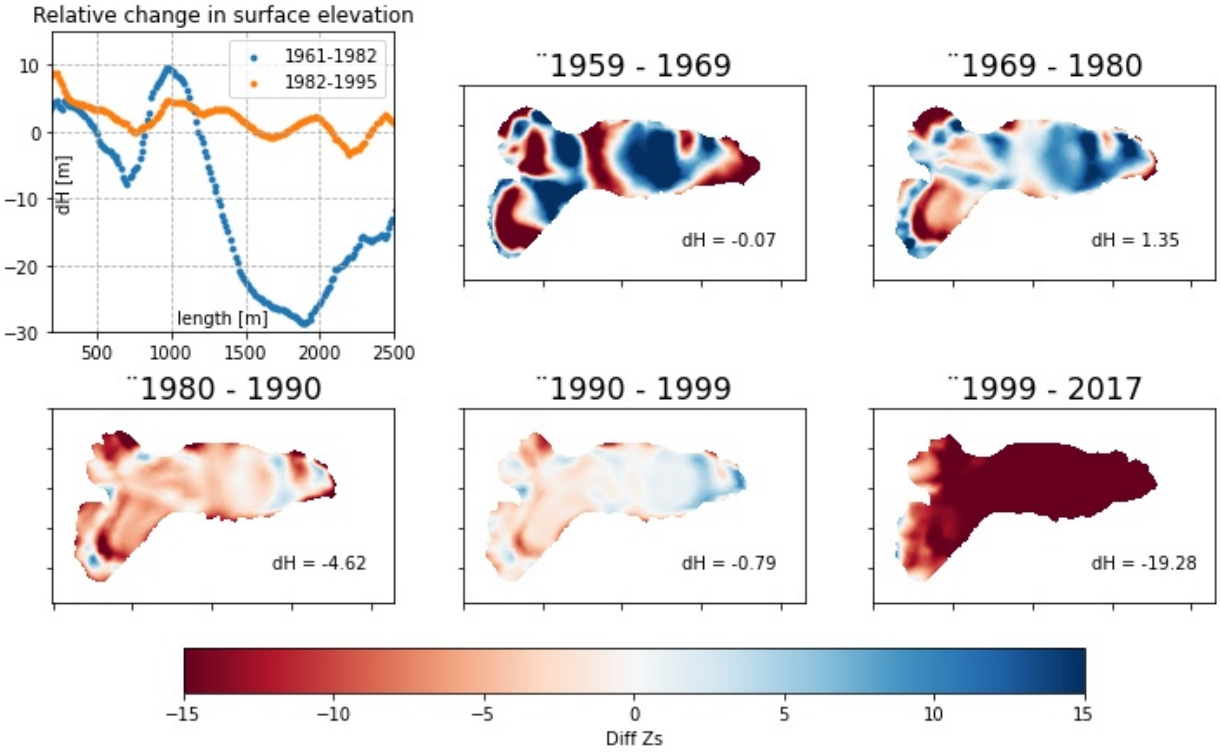

Figure 11: Surface elevation change for the periods 1961-1982 and 1982-1995 is plotted on the upper left. The elevation change is expressed in m. of ice in function of the length following the x-direction in Cartesian projection. Several plots show the surface elevation change in m. of ice between all the periods where a DEM is available. dH is the mean surface elevation change in m. of ice in the whole domain for each given period. All the plots use optim model.

6 Discussion

For numerical reasons, the whole simulation has been done with a unique rheology of the glacier but it is obvious that the glacier is polythermal. Thus, the inversion method and the sliding law taken into account focus on a dataset which is on the temperate layer to predict the rest of the basal rheology of the glacier. The qualitative method used (e.g using of velocity magnitude known at some points to validate the model) deserves a georeferencing of its points and possibly an increase in the number of data points. Also, inversion methods are not implemented with a Coulomb sliding law. Even if low speeds helps to limit the error, it would be justified to use a sliding law taken into account water pressure and cavitation due to the subglacial cavity resulting from the longitudinal sawtooth basal topography.
The implementation on mass balance in the model is very challenging. Even with a deep analysis of these latter, the response in the model can diverge from the observation. The derivation of the net balance from the altitude line already computed is debatable. Indeed, data are already subject to an interpolation when they are given by altitude band. With available data directly at stakes, a deeper analysis could be carrying out to deduce the relation. Moreover, there is no methodology attach to the mass balance measurements over the time. But it is obvious that few methods has been used. Thus, a data re-analysis (as it was done for Mårmaglaciären, 25 km N.W from TRS) to standardise these latter could give a better trust in.
The only variable correlated to mass balance is the altitude, but none of climate information is directly related to the model which can lead to important expansion/retreat of the glacier

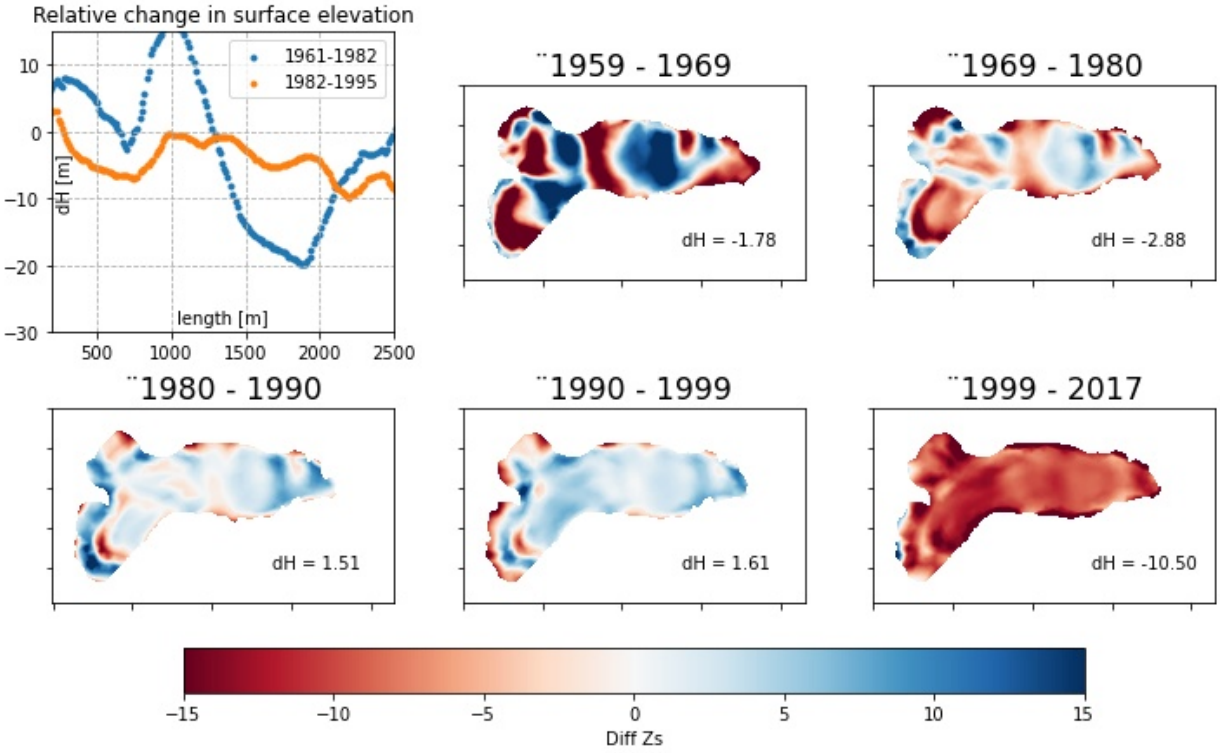

Figure 12: Surface elevation change for the periods 1961-1982 and 1982-1995 is plotted on the upper left. The elevation change is expresed in m. of ice in function of the length following the x-direction in cartesian projection. The other plots show the surface elevation change in m. of ice between all the periods where a DEM is available. dH is the mean surface elevation change in m. of ice in the whole domain for each given period. All the plots use R2 model.

modelled at some pretty stable climatic conditions (Figure 10). TRS has a long time series of climate data (temperature and precipitation) very close to Storglaciären. A multiple regression using these series would be a good way to include climate information. In addition it would provide great knowledge for a future model of glacier evolution.
Finally, yearly changes of the glacier can be observed at a small scale, especially for surface change or even more retreat of the glacier (length change at the bottom). The numerical issues of the model has constrained to increase the mesh size. As a result, small scale effects are not reproduced (with the mesh size of 100 m, a retreat of 100 m is needed to see it the model) and can affect the glacier as a larger scale in long term simulation.

7 Conclusion

The present study explored the FEM Elmer-Ice applied to the past evolution of Storglaciären (1959-2018), Swedish glacier. The numerical model shows a good ability to reproduce past changes by implementation of rerevored mass balance.

First, the presence of TRS as well as the various studies around are a major asset for the model. The DEMs are frequent over study time and allow a high resolution of the initial model (thickness, shape of the glacier) in addition of the comparison tools that can be use.
Despite the longest mass balance records of the glacier, velocity data remains really poor and badly distributed (only one dataset on a specific area). GPS position report of used for mass

balance record could be easily carry out and very useful to better understanding the flow of the glacier.
Surface velocity data is also essential in numerical glacier modelling to understand the subglacial flow (inversion methods). To overcome this lack of data, a new inversion method was tested in Elmer based on a correlation function depending of space. The auto-covariance length scale (*range* parameter in the model) is taken as the mean thickness of the glacier and the prior is defined as $C = 0.0275$ after a pre-simulation sensitivity study. The standard deviation (*std* on the model) has been found at $std = 5e - 03$ to match the model with the observation and reproduce the magnitude of the velocity known at some other points (such as maximal surface horizontal velocity of 21 $m/year$). The initial guess is extremely important to get a well-distributed surface velocity and avoid divergent optimised coefficient values at some points. A qualitative preliminary study to understand the glacier flow is highly recommended.
From this inversion, the idea was to take into account the water pressure in a second phase by converting Weertman friction law in Coulomb regularized friction law. However, the physical assumptions to make it mathematically solvable, was made for saw-tooth bedrock ice sheet, corresponding to $q = 1$ (glacier-type dependant parameter). Thus, applied to the alpine glacier with ellipsoidal bedrock of this study, the results are not conclusive. With the right parameter ($q = 2$ for ellipsoidal bedrock), the equation no longer has a unique solution and cannot be implemented in this way.
An other solution of taken into account water pressure, would be to explore the rheology of the glacier and be able to implement it directly in the model.
On the other hand, not taken into account water pressure is an acceptable assumption in this study because the surface velocity of the glacier is pretty low.

The most import source of uncertainty is the mass balance input in the model. Indeed, even if data are available, it was challenging to find a good relation fitting in the model. The choice was to use only elevation as a mass balance variable and explore different methods with linear and polynomial relations. Although a curvature is observed at the extremity of the glacier, linear relation shall apply. This curvature varies enormously from a year to an other depending of the ELA and tends to be less pronounced with the retreat of the glacier these last decades. This makes it complex to chose one model and a combination is better. This is also due to a lack of data (only altitude range of net balance is available and already interpolated), which shows the necessity to undertake a protocol-based re-analysis of the data.
Even though the second order polynomial regression gives a good fit of the volume lost of the glacier, the combination of linear methods (mean method, differentiation method and linear regression) is the one selected in this study because the retreat of the glacier this last few decades is much better simulated. This is related to the previous analysis showing the curvature reduction (linearization of the function).

Future climate and ice sheet modelling scenarios show a trend towards increasing glacier retreat especially in the study area. By adding climatic variables such as rainfall and temperature, this diagnostic numerical model of Storglaciären can be used to project the future of this glacier as well as many others in the surrounding area which together make the region a major focus of interest in climate.

8 Tarfala research station

TRS is Sweden's only research station located in a alpine arctic environment. Its proximity to the biggest glaciers of Sweden and the highest peak of Sweden (Kebnekaise) make the station engages both the general public and researchers across the globe.
Historically, this is an area of interest since the beginning of the 19th century and the first cabin was built in 1948 when the mass balance measurements has began. Then, the station grew up to be a field station for various geosciences research in an arctic alpine landscape. More recently the focus was on the education allow TRS to be a teaching place as well.

The station is open at the beginning of the spring to carrying out the winter mass balance with a reduced on-site staff. Then the station is closed almost 2 months to open again at the end of June for the summer research as well as summer courses.During the summer season, various courses focus on environmental sciences applied to arctic alpine environment are given in TRS, allowing to welcome few guests groups in the station all along the season (capacity of 28 guests maximum). To manage the fieldwork and the smooth running of the station when there are guests, a strong team is needed, made up as follows :

- 1 station director
- 1 station manager
- 2 field assistants
- 1 technical assistant
- 1 cook

Additional visitor can take part of the staff team for a short period and it was my case for this internship. Indeed, a visit at TRS has been planned for the month of July, in order to help on the fieldwork, see the glacier studied for the internship and discover the world of research in a station.

I was able to take part in the following tasks in the field (see appendix A for pictures):

- Mass balance statement on Storglaciären
- Discharge measurements via tracer dilution method (fluorescine) and salt dilution
- Recording temperatures in a glacial lake

As a member of the staff, my function was also to work with each other in everyday tasks necessary for the operation of the station. Finally, the visit at TRS was at the end of the internship and a large part of the schedule has been assigned to completing the simulation, formating the results and write the present report as well as the scientific article to be published.

A Stockholm University organisation chart

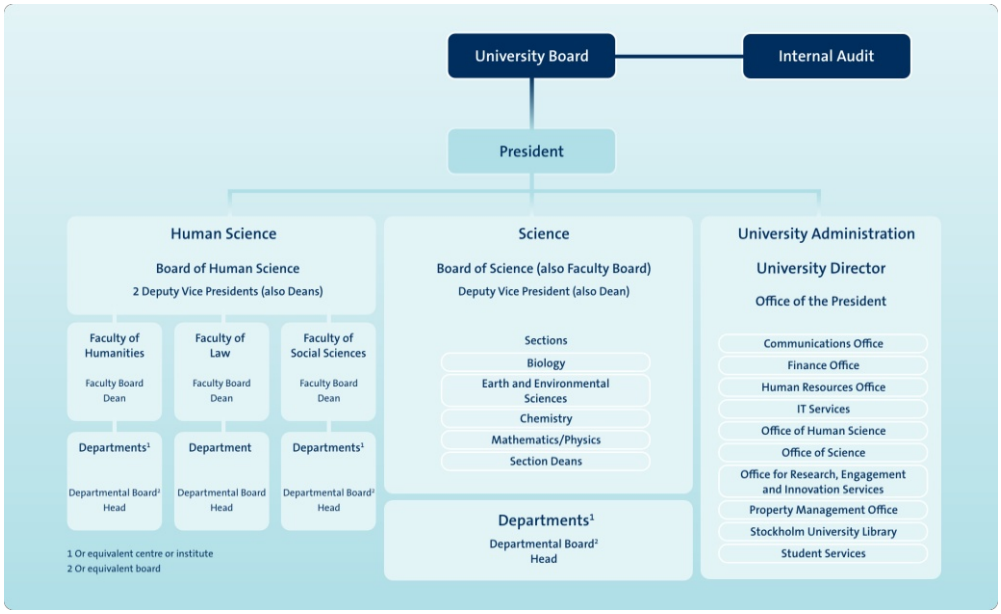

Figure 13: Organization chart of SU

B Weertman friction law to Coulomb

Regularized Coulomb law

Coulomb sliding function is expressed as the following :

$$\tau_b = C \cdot N \left[\frac{\chi \cdot u_b^{-n}}{(1 + a \cdot \chi^q)} \right]^{\frac{1}{n}} \cdot u_b \tag{15}$$

$$a = \frac{(q-1)^{q-1}}{q^q} \tag{16}$$

$$\chi = \frac{u_b}{C^n N^n A_s} \tag{17}$$

Standard linear Weertman as used in Elmer/Ice inversions (see 4.3.2):

$$\tau_b = 10^{\beta} u_b \tag{18}$$

Make the following assumptions:

$$q = 1, \tag{19}$$

$$n = 3, \tag{20}$$

$$C = 1. \tag{21}$$

Then equation 15 becomes

$$\tau_b = N \left[\frac{\chi u_b^{-3}}{1 + \chi} \right]^{1/3} u_b, \tag{22}$$

which can be rearranged to give

$$\chi = \frac{1}{\left(\frac{N}{\tau_b}\right)^3 - 1}. \tag{23}$$

Also, equation 17 becomes

$$\chi = \frac{u_b}{N^3 A_s}. \tag{24}$$

Then equations 23 and 24 can be combined to give

$$A_s = \frac{u_b}{\tau_b^3} - \frac{u_b}{N^3}. \tag{25}$$

Then we can substitute the expression for τ_b used in the inversions to give

$$A_s = \frac{1}{10^{3\beta} u_b^2} - \frac{u_b}{N^3}, \tag{26}$$

where β is the optimised variable from inversion4.3.2. This is the equation used to calculate A_s. β and u_b come from the inversion. N can be based on the hydrostatic assumption or Elmer's computed normal stress can be used, but in either case the largest uncertainty comes from whatever assumption is made to calculate water pressure.

Conversion

For the Weertman parameter, A_s the following relation is used:

$$A_s = u_b^{1-n} \cdot 10^{-n\beta}. \tag{27}$$

The reference value, A_{s0}, is taken as the average value over the whole domain.
With this given values, a local reference value of χ_0 can be computed using the sliding velocity and the effective pressure from the inversion.

$$\chi_0 = \frac{u_b}{N^n A_{s0}}. \tag{28}$$

In the very large limit for χ we can stick to a pure Coulomb interpretation

$$C = u_b \cdot 10^{\beta} \cdot N^{-1}. \tag{29}$$

Now, let's rovide more general version of equation 29 including dependence on A_s :

$$C^n = \frac{u_b \tau_b^n}{N^n (u_b - \tau_b^n A_s)} \tag{30}$$

$$C^n = \frac{u_b^n 10^{n\beta}}{N^n (1 - 10^{n\beta} u_b^{n-1} A_s)} \tag{31}$$

$$C = u_b \cdot 10^{\beta} \cdot N^{-1} \cdot (1 - 10^{n\beta} u_b^{n-1} A_s)^{-1/n} \tag{32}$$

This simplifies to equation 29 for $A_s = 0$.
We have seen in section 2.2 that n is considered as $n = 3$. Which lead to :

$$C = u_b \cdot 10^{\beta} \cdot N^{-1} \cdot (1 - 10^{3\beta} u_b^2 A_s)^{-1/3} \tag{33}$$

A Tarfala research station

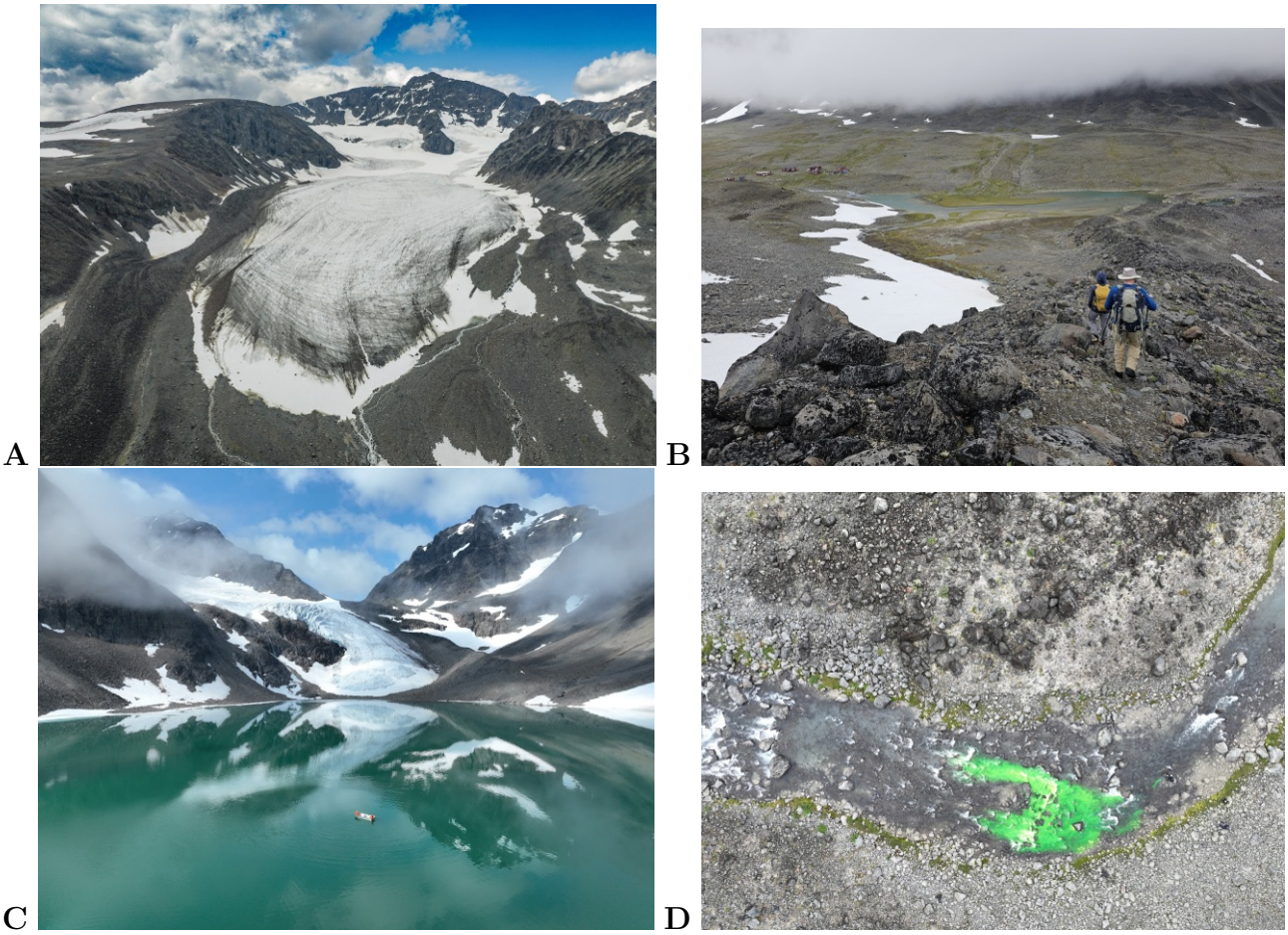

Figure 14: From the upper left to the lower right: A) Storglaciären from aerial view, glacier study in the present report B) TRS on the background photgraphed from the moraine of Storglaciären C) Tarfala lake from aerial view with the boat in the centre for temperature measurements D) Tarfalajokk from aerial view during discharge measurements with fluorescine.

References

[1] Rasmussen L. A. and Andreassen L. M.

[2] Blatter H. Albrecht O., Jansson P. Modelling glacier response to measured mass-balance forcing. 10.3189/172756400781819996. Annals of Glaciology, 31, 91-96, 2000.

[3] Helgi Björnsson H. Radio-Echo Sounding Maps of Storglaciären, Isfallsglaciären and Rabots Glaciär, Northern Sweden. 10.2307/520835. Geografiska Annaler. Series A, Physical Geography, 63, 225-231, 1981.

[4] C. J. van Der Veen. Fundamentals of Glacier Dynamics. volume 2. CRC Press, 2013-03-26.

[5] Howard C. Elman, David J. Silvester, and Andrew J. Wathen. 412Solution of Unsteady Navier–Stokes equations. In *Finite Elements and Fast Iterative Solvers: with Applications in Incompressible Fluid Dynamics*. Oxford University Press, 06 2014.

[6] De Rydt J. et al. Surface undulations of Antarctic ice streams tightly controlled by bedrock topography. 10.5194/tc-7-407-2013. The Cryosphere, 7, 407-417, 2013.

[7] Gagliardini et al. Finite-element modeling of subglacial cavities and related friction law. https://10.1029/2006JF000576. Journal of Geophysical Research, 112 (F2) F02027, 2007.

[8] Hooke Roger LeB. et al. A 3 year record of seasonal variations in surface velocity, StorglaciÄren, Sweden. 10.3189/S0022143000004561. Journal of Glaciology, 35, 235-247, 1989.

[9] Koblet T. et al. Reanalysis of multi-temporal aerial images of Storglaciären, Sweden (1959–99) – Part 1: Determination of length, area, and volume changes. 10.3189/172756405781812547. The Cryosphere, 4 333-343, 2010.

[10] Recinos B. et al. A framework for time-dependent Ice Sheet uncertainty quantification, applied to three West Antarctic ice streams. https://doi.org/10.5194/tc-2023-27. The Cryosphere, 2023.

[11] J.Ch. Gilbert and C. Lemaréchal. Some numerical experiments with variable-storage quasi-newton algorithms. Mathematical Programming, 42 407-435, 1989.

[12] Gudmundsson G. H. Analytical solutions for the surface response to small amplitude perturbations in boundary data in the shallow-ice-stream approximation. https://tc.copernicus.org/articles/2/77/2008/. The Cryosphere, 2, 77-93, 2008.

[13] Holmlund P. Holmlund Erik S. Constraining 135 years of mass balance with historic structure-from-motion photogrammetry on Storglaciären, Sweden. 10.1080/04353676.2019.1588543. Geografiska Annaler. Series A, Physical Geography, 101, 195-210, 2019.

[14] Cuffey KM and 4th Edn Paterson WSB. The Physics of Glaciers. Amsterdam: Academic Press Inc, 2010.

[15] Kurt M. Cuffey, W. S. B. Paterson. The Physics of Glaciers - 4th Edition. Oxford University Press, 07 2006.

[16] F. Pedregosa, G. Varoquaux, A. Gramfort, V. Michel, B. Thirion, O. Grisel, M. Blondel, P. Prettenhofer, R. Weiss, V. Dubourg, J. Vanderplas, A. Passos, D. Cournapeau, M. Brucher, M. Perrot, and E. Duchesnay. Scikit-learn: Machine learning in Python. *Journal of Machine Learning Research*, 12:2825–2830, 2011.

[17] Blatter Heinz Pettersson Rickard, Jansson Peter. Spatial variability in water content at the cold-temperate transition surface of the polythermal storglaciären, Sweden. `10.1029/2003JF000110`. Journal of Geophysical Research: Earth Surface, 109, 2004.

[18] Weertman.J. Stability of the junction of an ice sheet and an ice shelf. `https://10.3189/S0022143000023327`. Journal of Glaciology, 13 (67) 3-11, 1974.